Appl. Phys. A 90, 469–473 (2008)
DOI: 10.1007/s00339-007-4305-1

Applied Physics A
Materials Science & Processing

P. KUMAR
J. KUMAR
M. AHMAD
R. THANGARAJ✉

Effect of composition and light intensity on the electrical properties of Sn–Sb–Se glassy films

Semiconductors Laboratory, Department of Applied Physics, Guru Nanak Dev University, Amritsar 143005, India

Received: 30 March 2007 / Accepted: 21 September 2007
Published online: 31 October 2007 •

ABSTRACT Electrical and photoelectrical measurements have been performed on $Sn_xSb_{20}Se_{70-x}$ ($8 \leq x \leq 16$) glassy films. The dc activation energy, optical gap and photoconduction parameters show a typical variation near $x = 10$ composition indicating the occurrence of a rigidity percolation threshold in the present system. The photosensitivity increases with the increase in Sn content up to $x = 14$ and an abrupt decrease for $x = 16$ composition. Negative photoconductivity region have been observed in the higher temperature side for samples with $x = 10$ and 16. This system belongs to the type II category of photoconductors. The results are explained on the basis of a change in the density of localized states present in the mobility gap with the change in the composition.

PACS 71.20.Nr; 72.20.-I; 78.66.Jg; 81.05.Gc; 73.50.Pz

1 Introduction

The composition dependence of various properties of ternary chalcogenide glasses and films has been intensively investigated due to technologically important physical properties [1, 2]. Chalcogenide glasses exhibit unusual variation in the physical properties at two topological thresholds known as the rigidity percolation threshold (RPT) [2, 3], and chemical threshold (CT) [2]. The rigidity percolation threshold deals with the dimensionality and rigidity of the network, which occurs at an average coordination number $Z = 2.40$. However, at the chemical threshold, the chemical ordering is maximized with bonding being fully heteropolar. Thus, the measurements of various physical properties in the wide composition range can be used to develop a relation between the local structure, density, activation energy and transport properties etc. in a glassy system. These studies are also important for determining the microscopic and macroscopic structure and hence to understand the structure–property correlation, resulting in better materials for device applications.

The investigation of steady state and transient photoconductivity is a valuable tool for the study of the transport mechanism and defect states in a semiconductor [4–6]. On the basis of temperature dependent steady state photoconductivity measurements, photoconductors can be classified in two categories: type I and type II semiconductors [4]. Type I semiconductors exhibits a maxima in photoconductivity at a specific temperature T_m with the magnitude generally larger than the dark conductivity for $T < T_m$ and smaller than the dark conductivity for $T > T_m$. While in type II semiconductors, the photoconductivity maxima is absent, the photocurrent increases slowly and monotonically with increasing temperature and it is in general much less than the dark current. In the same temperature region for a sample, illumination causes the total current to decrease to a level that is less than the dark value. This phenomenon is typically known as negative photoconductivity [4]. So, these measurements are useful in understanding the compositional effects on the recombination mechanism and localized states present in the mobility gap of theses materials.

The study of Sn–Sb–Se glasses has been of recent interest due to their small glass-forming region [7, 8] as compared to other alloys from the IV–V–VI ternary system, where light mass elements were used. The composition variation may lead to the modification of the network structure as described by the relative change in the concentrations of the different cluster units. Thus, these studies could directly be related to the relative variation in the concentrations of different network building cluster units in a system [9]. The photoconductivity studies in a wide composition region have been of great importance in finding the influence of these percolating clusters on the glass network. Therefore, a systematic study of the photoelectrical properties of this system is required for better understanding of the physics of these materials. In view of the above, we have attempted to study the effect of Se replacement with metallic Sn on the photoconduction process in this Sb–Se system. The occurrence of rigidity transitions and their effect on the defect states is used to discuss the present results.

2 Experimental details

Bulk glasses of $Sn_xSb_{20}Se_{70-x}$ ($8 \leq x \leq 16$) system were prepared by conventional melt quenching techniques as described elsewhere [8]. The deposition was carried out in a high vacuum system (HINDHIVAC coating unit, Model no. 12A4D) at a pressure of 10^{-5} mbar. The well-cleaned glass slides kept at room temperature as substrates and the source material taken in molybdenum boats were used

✉ Fax: +91-183-2258819, E-mail: rthangaraj@rediffmail.com

for the deposition. The thickness of the films was measured by the Tolansky interference method and found to be ∼ 350 nm. The differential scanning calorimetric (DSC) studies [8] were carried out to confirm the glassy nature of these materials. XRD was performed to ascertain the amorphous nature of the thin film samples. The optical transmission spectrum was recorded at room temperature using an UV-VIS spectrophotometer in the wavelength range 500–1100 nm.

The Al electrodes (electrode gap ∼ 2 mm) in co-planar geometry were used for electrical and photoelectrical measurements. The sample was mounted in a metallic cryostat with a transparent window having an arrangement for varying the temperature. The dc conductivity measurements were carried out in the temperature range 253–343 K in a running vacuum of $\sim 10^{-4}$ Torr. The current was measured using a digital picoammeter (DPM-111, Scientific equipment, Roorkee). For photoconductivity measurements, the sample was illuminated using a 500 W tungsten halogen lamp (Halonix, India) with an infrared filter. By changing the distance between the sample and light source, the intensity was varied during the experiment. The intensity of light was measured with a digital lux meter (LX-101, Taiwan). The photocurrent (I_{ph}) is obtained after subtracting the dark current (I_d) from the current measured in the light.

3 Results and discussions

3.1 *Dark conductivity and optical gap*

The temperature dependent conductivity studies were carried out well below the respective glass transition temperatures to avoid the micro-crystallization of the constituents on the higher temperature side. The electrical conductivity of thin films of $Sn_xSb_{20}Se_{80-x}$ ($8 \le x \le 16$) as a function of temperature (253–343 K) is shown in Fig. 1. The increase in dark conductivity with the increase in temperature is observed for all the samples (Fig. 1). The linearity of the $\ln\sigma$ against $1/T$ indicates that the conductivity is thermally activated in the studied temperature region. The conductivity (σ) obeys the relation: $\sigma_d = \sigma_0 \exp(-\Delta E/kT)$, where σ_0 is a pre-exponential factor, ΔE is the activation energy and k is the Boltzmann constant. The values of σ_0 and ΔE have been estimated from the intercept and slope of the curve by using least square curve fitting and are summarized in Table 1. It follows from the table that the value of ΔE is 0.37 eV for $x = 8$, which increases to 0.49 eV for $x = 10$ and thereafter a decrease in the activation energy has been observed. The optical absorption coefficient (α) was determined from the transmission spectrum as: $\alpha = (1/d)\ln(100/T)$, where T is the transmittance and d is the thickness of the film. Figure 2 shows the spectral variation of the absorption coefficient in the 750–1000 nm wavelength region. From the Tauc plots between $(\alpha h\nu)^{1/2}$ versus $h\nu$, the optical gap (E_0) for all the compositions have been evaluated and summarized in Table 1. The optical gap follows the same trend as that observed for the dc activation energy.

x	Z	R-value	T_g (K)	σ_{303} (S cm^{-1})	E_{dc} (eV)	σ_0	E_0 (eV)
8	2.36	1.56	409.0	2.34×10^{-4}	0.37	2.7×10^{2}	1.11
10	2.40	1.40	426.5	8.35×10^{-5}	0.49	1.2×10^{5}	1.12
12	2.44	1.26	434.9	1.05×10^{-4}	0.44	4.7×10^{3}	1.10
14	2.48	1.14	448.9	1.34×10^{-4}	0.43	2.5×10^{3}	0.97
16	2.52	1.03	460.2	1.90×10^{-4}	0.41	1.7×10^{3}	0.96

TABLE 1 The average coordination number (Z), R-value, glass transition temperature (T_g), and electrical and optical parameters, with composition for Sn–Sb–Se glassy semiconductors

3.2 *Temperature dependent photoconductivity*

Figure 3a,b shows the temperature dependence of the steady state photoconductivity at two different intensities 100 lux and 1200 lux respectively, for all the samples. It is clear from the figure that photoconductivity increases ex-

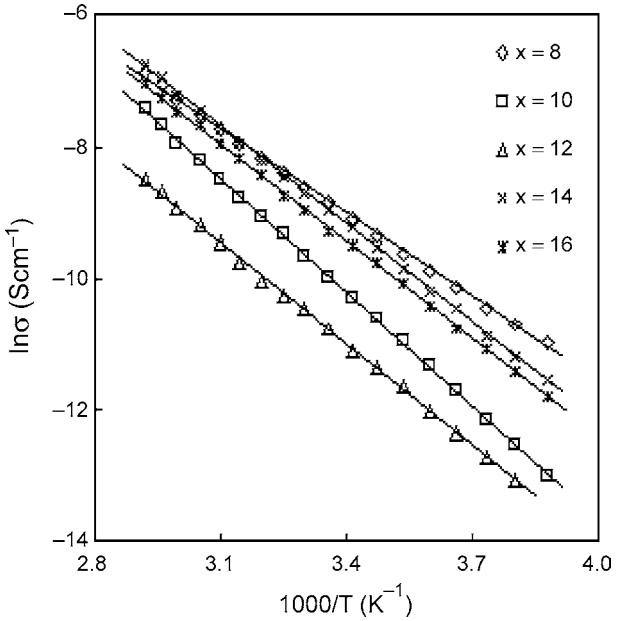

FIGURE 1 Temperature variation of dark conductivity ($\ln\sigma$) for $Sn_xSb_{20}Se_{80-x}$ films

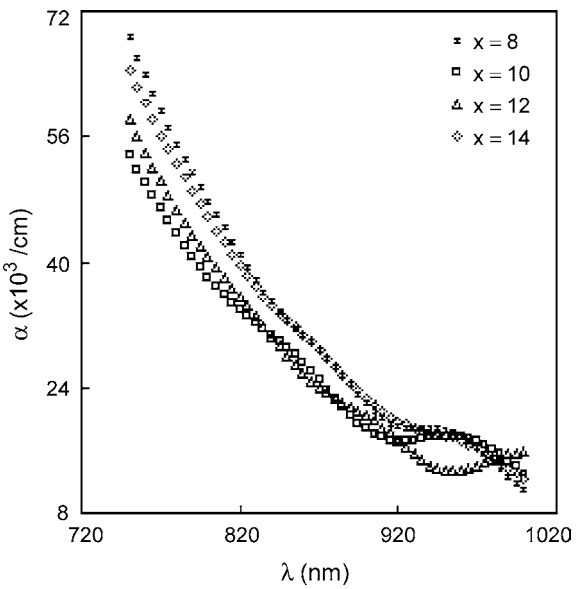

FIGURE 2 Spectral dependence of the absorption coefficient (α) for $Sn_xSb_{20}Se_{80-x}$ films

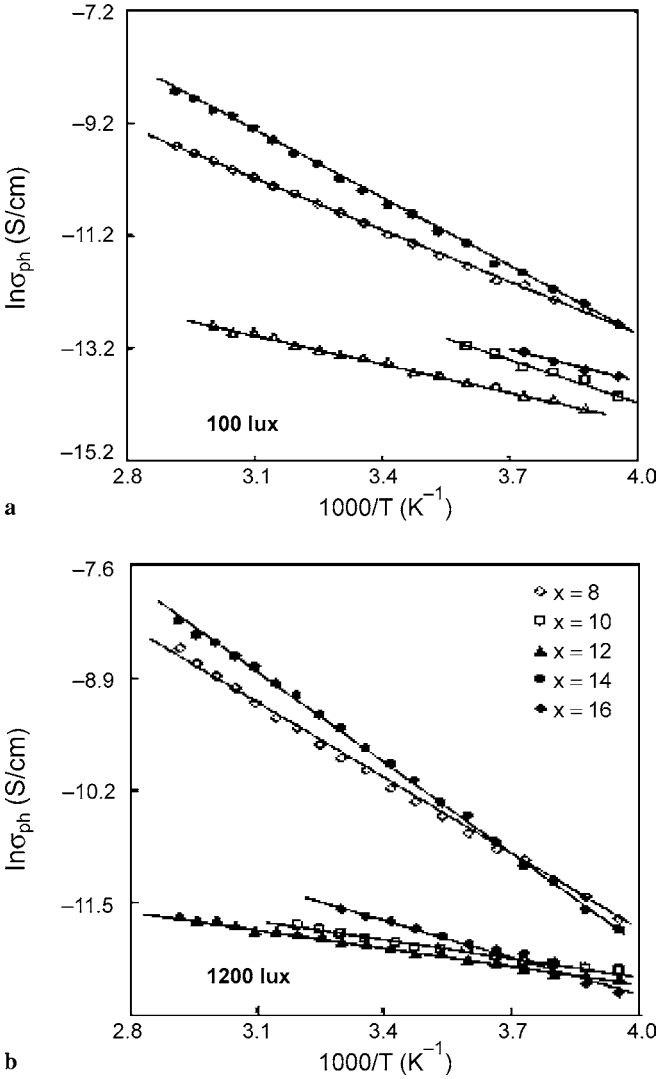

FIGURE 3 The variation of photoconductivity with the inverse temperature at different light intensities (**a**) 100 lux and (**b**) 1200 lux for $Sn_xSb_{20}Se_{80-x}$ thin films

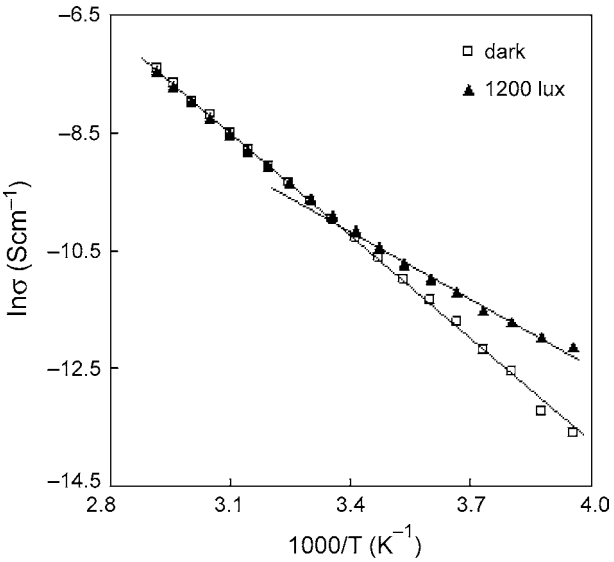

FIGURE 4 Variation of dark conductivity and total conductivity at 1200 lux with inverse temperature for $Sn_{10}Sb_{20}Se_{70}$ films

x	E_{dc} (eV)	E_{ph} (eV)		S ($\times 10^{-2}$)	γ
		100 lux	1200 lux		
8	0.37	0.27	0.25	6.4	0.61
10	0.49	0.21	0.06	10.4	0.52
12	0.44	0.24	0.08	12.4	0.73
14	0.43	0.27	0.15	17.3	0.85
16	0.41	0.30	0.21	3.2	0.94

TABLE 2 Some photoelectrical parameters for the Sn–Sb–Se glassy film samples

ponentially in the measured temperature range (253–343 K). The region of photoconductivity measurement was extended to higher temperatures as we increased the intensity of light. Figure 4 shows the variation of dark conductivity and total conductivity at 1200 lux with inverse temperature for $Sn_{10}Sb_{20}Se_{70}$ films. When the value of the total current is less than the equilibrium dark current value it then gives a negative value for the photocurrent. In the present case, the total conductivity in the presence of light is less than that of the dark conductivity in the higher temperature range. This region extends to higher temperatures as the light intensity increases. Also, the photoconductivity is much less than the dark conductivity, while no maxima in the photoconductivity with temperature were observed. This indicates that this Sn–Sb–Se system belongs to the type II category of the photoconductors [4].

From these plots, the value of activation energies for photoconductivity with the light intensity and composition has been calculated. These values are summarized in Table 2. The activation energy for photoconductivity is much smaller than the dark current activation energy and it decreases as we increase the light intensity. This is in accord with a model of Simmons and Taylor with distributed set of defect states [10]. In this model, there is a continuous distribution of localized states present in the mobility gap of the material. This model provides the information for the energy location of discrete sets of localized states (D^+ and D^-) in the mobility gap. These centers D^+ and D^- act as discrete traps for the photogenerated electrons and holes, thereby giving rise to neutral (D^0) sites which, due to polaronic lattice deformation, produce energy levels roughly midway between the band edges and the Fermi level. The position of these localized states depends on the composition and light intensity. Also, the Fermi level splits into electron and hole quasi Fermi levels, and moves towards the valence band for holes (E_{Fp}), and towards the conduction band for electrons (E_{Fn}), with increasing light intensity [4, 10]. The increase in the light intensity further facilitates the shift due to the increase in the number of photogenerated carriers or carrier mobility, results in the decrease in E_{ph} value.

3.3 *Photosensitivity*

The variation of normalized photocurrent I_{ph} with time t during and after the illumination is shown in Fig. 5. All the samples show the same trend. The initial rise and decay, of the photocurrent is fast but thereafter becomes slow. The photodegradation has not been observed in the present system,

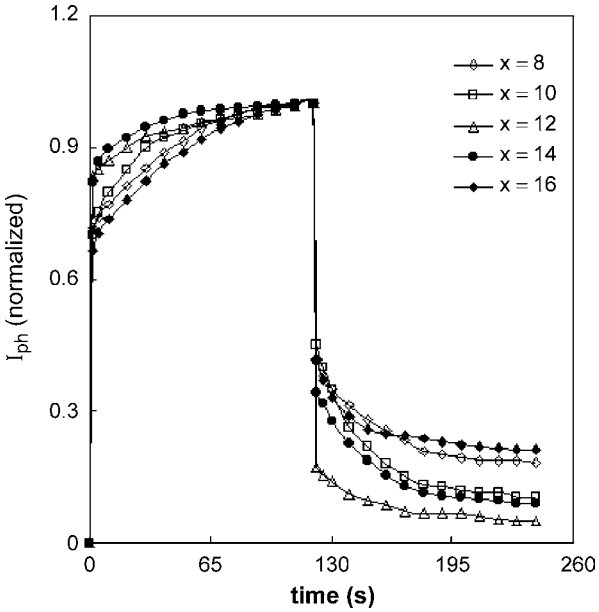

FIGURE 5 Rise and decay of normalized photocurrent with time at room temperature and fixed light intensity (1200 lux) for $Sn_xSb_{20}Se_{80-x}$ ($8 \le x \le 16$) thin film samples

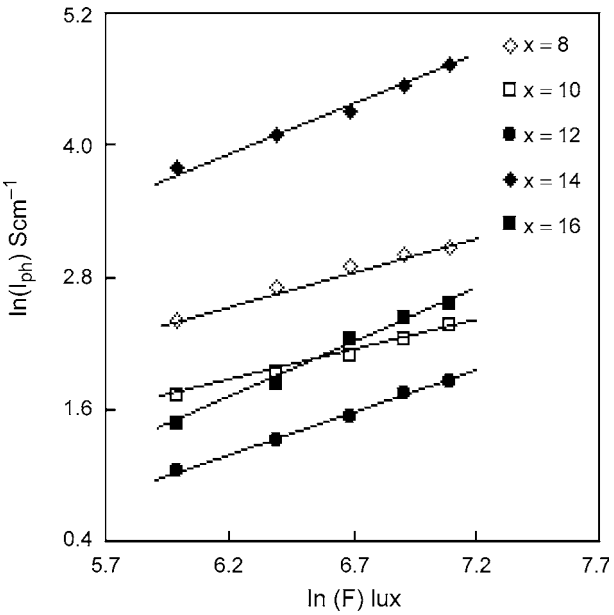

FIGURE 6 Dependence of photocurrent on light intensity for Sn–Sb–Se films at room temperature

as with narrow gap chalcogenide films [11]. The photocurrent decays very slowly for $t > 100$ s after the illumination is stopped and the persistent current is slightly more than the initial dark current value. In these materials having traps in the mobility gap, the recombination time of the carriers is the same as the carrier lifetime when the free carrier density is more than the trapped carrier density. If the free carrier density is much less than the trapped carriers, the recombination process is dominated by the rate of trap emptying and is much larger than the carrier lifetime, resulting in the slow decay.

In order to simplify the analysis of the photoconductivity kinetics, this persistent photocurrent is subtracted from the total photocurrent to obtain I_{ph}. This type of behavior has been observed in many other chalcogenide semiconductors [12, 13]. An important parameter in the photoconductivity measurements is the photosensitivity ($S = I_{ph}/I_d$), which indicates the effect of composition, light intensity and temperature on the defect state density in the gap. Table 2 summarizes the calculated values of S at room temperature for all the samples.

There is a large decrease in the photosensitivity (S) at $x = 10$ and thereafter the value increases up to $x = 14$ and finally it decreases sharply for the composition with $x = 16$. The maximum in the value of S has been observed for $x = 14$ (Table 2). The value of S depends on the lifetime of the excess carriers, which in turn depends on the density of localized states in a particular material. The higher the density of defect states, the lower will be the life time, as these defect states act as recombination centers in the presence of light [14, 15]. Therefore the change in the photosensitivity could be due to the change in the defect state density with the composition.

3.4 *Effect of light intensity*

The effect of light intensity (F) on the photoconductivity at room temperature (308 K) was studied for all the samples. Figure 6 shows the plots of ln I_{ph} versus ln F for all the samples. These plots indicate that σ_{ph} increases with intensity following the power law: $I_{ph} \propto F^{\gamma}$, where γ, is the exponent and the value of it is determined by the recombination mechanism [4]. The value of $\gamma \approx 0.5$, indicates a bimolecular recombination process, whereas $\gamma \approx 1.0$ indicates a monomolecular mechanism. If the value of the exponent lies between $0.5 \le \gamma \le 1.0$, then there is continuous distribution of traps. The exponent γ has been calculated for all the samples and summarized in Table 2. The value of the exponent varies between (0.52–0.94) with composition, indicating a change in the recombination process with the change in composition. The value of γ, first decreases to 0.52 for $x = 10$, giving the bimolecular recombination and then increases with composition leading to the continuous distribution of traps. Present results can be understood by taking into account the change in the density of localized states with the change in the average coordination number (Z) as discussed in the next section.

3.5 *Effect of composition*

Theses results indicate a strong dependence of the photoconduction parameters on the composition or average coordination number with the increase in Sn content. In this section, the results are discussed by considering the occurrence of topological thresholds viz RPT and CT in the present ternary system. The average coordination number (Z) has been calculated by considering the coordination number of 4, 3 and 2 for Sn, Sb and Se respectively [8]. For the present glassy system ($Sn_xSb_ySe_z$), the average coordination number was calculated as $Z = (4x + 3y + 2z)/(x + y + z)$. The present measurements indicates a minimum or maximum in the properties at $Z = 2.40$ ($x = 10$), which is associated with the rigidity of floppy transition. With further increase in Sn content, the change in the photoconduction parameters are associated

with the approaching of the chemical threshold in the present system. For this, the R-value for $Sn_xSb_ySe_z$ glass is calculated as: $R = 2z/(4x + 3y)$. The R-value represents the ratio of the covalent bonding possibilities of the chalcogen atoms to the covalent bonding possibilities of the non-chalcogen atoms [16, 17].

Thus, the value of $R = 1$ represents the case of the existence of only heteronuclear bonds, which indicates the occurrence of the chemical threshold [15]. The Z and R-values are summarized in Table 1. In between these two thresholds, the occurrence of phase separation has been observed for many chalcogenide systems [2]. The occurrence of phase separation is due to constraint of the mixing of different molecular clusters leading to the increase in the heterogeneity and hence, an increase in the defect state density in the gap. Thus, the increase in the glass transition temperature with the decrease in thermal stability [8] and optical gap are associated with the phase separation in the Sn–Sb–Se glassy system.

The values of ΔE and E_{ph} do not follow the same trend. The variation in the value of E_{ph} is opposite to that of ΔE, as there is a large decrease in the E_{ph} value at $Z = 2.40$ as compared to the increase in the ΔE value. Thus, the nature of the photoinduced effects changes as Z increases to the $Z = 2.40$ value. The behavior of the photoinduced relaxation of the network, which is different for compositions before the $Z = 2.40$ value, and in regions where the phase separation occurs. The small changes in the values of ΔE and E_{ph} (100, 1200 lux) for $x = 16$ can be associated with the chemical threshold for the present system.

These results can also be analysed by considering the nucleation of different cluster units as the value of Z increases. In these glasses, growth of chemically dissimilar clusters with different atomic arrangements and structural units are taking place with the increase in the Sn content [9]. The constraint of mixing of different molecular fragments or clusters, leads to an increase in the surface dangling bonds and increased density of defect states in the mobility gap. Therefore, the nucleation and growth of these clusters lead to a change in the microscopic structure and hence, a change in the density of defect states with the increase in Z. The phase separation and cluster boundary defects introduce states in the mobility gap, revealing the effect of composition in the present glassy semiconductors.

4 Conclusion

Steady state and transient photoconductivity measurements have been performed on amorphous thin films of Sn–Sb–Se as a function of temperature, light intensity and illumination times. The temperature dependence of their photoconductivity indicates that these semiconductors belong to the type II photoconductors with single activation energy. The change in the activation energy for dark conductivity as well as for photoconductivity, recombination mechanisms and photosensitivity, has been observed with an increase in Sn content.

ACKNOWLEDGEMENTS The authors wish to thank Dr. Atul Khanna, for his valuable help in the UV-VIS spectroscopy and helpful discussions during the course of the experiment.

REFERENCES

1 K. Morigaki, *Physics of Amorphous Semiconductors* (Imperial College Press, London, 1999)
2 P. Boolchand, *Insulating and Semiconducting Glasses* (World Scientific, Singapore, 2000)
3 J.C. Philips, M.F. Thorpe, Solid State Commun. **53**, 699 (1985)
4 R.H. Bube, *Photoelectrical Properties of Semiconductors* (Cambridge University Press, Cambridge, 1992)
5 N. Qamhich, G.J. Adriaenssens, J. Non-Cryst. Solids **292**, 80 (2001)
6 M.S. Iovu, S.D. Shutov, V.I. Arkhipov, G.J. Adriaenssens, J. Non-Cryst. Solids **299–302**, 1008 (2002)
7 A.B. Adam, S. Sakrani, Y. Wahab, J. Mater. Sci. **40**, 1571 (2005)
8 P. Kumar, K.S. Bindra, N. Suri, R. Thangaraj, J. Phys. D Appl. Phys. **39**, 646 (2006)
9 M. Shurgalin, V.N. Fulfyigin, E.G. Anderson, J. Phys. D Appl. Phys. **38**, 4037 (2005)
10 J.G. Simmons, G.W. Taylor, J. Phys. C Solid State Phys. **7**, 3051 (1974)
11 K. Hayashi, Y. Hikida, K. Shimakawa, S.R. Elliott, Philos. Mag. Lett. **76**, 233 (1997)
12 R.M. Mehra, A. Ganjoo, P.C. Mathur, J. Appl. Phys. **75**, 7334 (1994)
13 N. Manikandan, B.H. Sharmila, S. Asokan, Appl. Phys. A **81**, 1313 (2005)
14 K. Shimakawa, S. Inami, S.R. Elliott, Phys. Rev. B **42**, 118 (1990)
15 K. Shimakawa, A.V. Kolobov, S.R. Elliott, Adv. Phys. **44**, 475 (1995)
16 L. Tichy, H. Ticha, Mater. Lett. **21**, 313 (1994)
17 G. Saffarini, Appl. Phys. A **74**, 283 (2002)